N O T I C E

THIS DOCUMENT HAS BEEN REPRODUCED FROM MICROFICHE. ALTHOUGH IT IS RECOGNIZED THAT CERTAIN PORTIONS ARE ILLEGIBLE, IT IS BEING RELEASED IN THE INTEREST OF MAKING AVAILABLE AS MUCH INFORMATION AS POSSIBLE

NASA Technical Memorandum 81338

MLS Vertical Guidance and Navigation for a STOL Airplane Landing on an Elevated STOLport

David N. Warner, Jr.

November 1981

National Aeronautics and
Space Administration

NASA Technical Memorandum 81338

MLS Vertical Guidance and Navigation for a STOL Airplane Landing on an Elevated STOLport

David N. Warner, Jr., Ames Research Center, Moffett Field, California

NASA
National Aeronautics and
Space Administration

Ames Research Center
Moffett Field, California 94035

MLS Vertical Guidance and Navigation For a STOL Airplane Landing on an Elevated STOLport

David N. Warner, Jr.

SUMMARY

In contrast to CTOL landing operations, STOL airplanes landing on short STOLport runways typically begin the flare maneuver before reaching the runway surface. Vertical guidance procedures have been developed to allow an autoland flight control system for a STOL airplane to use Microwave Landing System (MLS) signals as altitude and sink rate references for flare initiation, with a transition to radar altimeter after the airplane is over the runway. The implementation has minimum impact on the control system and landing performance. Data is presented which show validation of the concepts in a simulator.

INTRODUCTION

Several papers have been written about the use of the time referenced scanning beam Microwave Landing System (MLS) for conventional take off and landing (CTOL) approaches and automatic landings (references 1 and 2). In these studies, flare was initiated after crossing the threshold since the MLS approach elevation antenna was sited several hundred feet from the runway threshold. Thus altitude and altitude rate were computed from MLS elevation and precision distance measuring equipment (DME) data until the airplane reached the runway and then the altitude reference was transitioned to a radar altimeter prior to initiation of the flare. This procedure provided a highly accurate altitude and altitude rate reference for use in the flare algorithm to provide safe, accurate flare initiations and automatic landings.

To investigate the use of MLS for automatic landings of powered lift vehicles, a flight test was conducted with the Augmentor Wing Jet STOL Research Airplane (AWJSRA), references 3 and 4. This is a powered-lift STOL research airplane which has been equipped with a digital flight control system, reference 5. The autoland control laws were similar to those used in CTOL transports but were tailored to the unique characteristics of the STOL test airplane. At the airport where the STOL autoland flight tests were conducted, more than 1200 meters (4000 ft) of smooth runway were available in front of the marked STOLport. As in the CTOL studies, this long underrun provided ample opportunity to converge the radar altimeter based sink rate filter. This stable sink rate, along with the accurate altitude from the radar altimeter, provided a high quality reference for the flare and automatic landing.

In general, since STOL landing situations typically require that the glide path intercept point (GPIP), and therefore the MLS approach elevation antenna, be near the threshold to minimize runway length (reference 6), most

STOLports will not have underrun areas which are long enough to provide an acceptable radar altimeter signal during the entire flare. This siting arrangement requires that flare initiation occur before reaching the runway threshold and therefore without the use of radar altimeter. Indeed a major discontinuity in radar altitude may occur, as at the end of an elevated STOLport (reference 6).

The use of MLS and the late transition from MLS to radar altimeter pose three major questions: (1) what procedure should be used to transition from MLS derived altitude and sink rate to radar altimeter derived altitude and sink rate for use in the flare law without adversely affecting the automatic flare performance; (2) does the MLS system proposed for CTOL have the azimuth, elevation and DME accuracy needed for STOL operations, and if not, what accuracies are required; and (3) does the resulting system produce repeatable, consistent performance that will be acceptable to pilots.

In order to answer these questions, a technique for transitioning from MLS to the radar altimeter after the airplane is over the threshold and during the flare was developed and evaluated in the presence of varying MLS bias errors using a fixed based simulation of the Augmentor Wing Jet STOL Research Airplane. This report describes the technique and presents the results of the simulation tests. Data is presented which show the variations of touchdown distance and sink rate at touchdown as a function of MLS errors.

Lateral guidance from MLS azimuth does not appear to pose any significant problems for STOL Operations (reference 4) and is not discussed. Although the study focused on an autoland system, the vertical navigation and guidance methods are equally applicable for flight director approaches and flare monitoring systems.

PROCEDURES

Simulator Description

The simulation facility consists of (1) an EAI 8400 digital computer to simulate the aircraft, STOLport, and MLS system, (2) a digital flight control system, (3) a simulation cockpit with standard aircraft instruments along with an advanced mode select panel and electronic CRT displays, and (4) data conversion interfaces for data reformatting between the simulation computer and the flight control computer and the cockpit instruments.

The STOL aircraft modeled in the simulation computer is a modified deHavilland C-8A Buffalo airplane, Figure 1. It has two turbofan engines which provide flow through augmentor flaps and ailerons and through vectorable exhaust nozzles. This system allows the airplane to fly at 70 knots on glideslope approaches of -7.5 degrees flight path angle. All control surfaces and lift control devices are controlled by servos from the digital flight control system. More complete descriptions of the airplane and its operating characteristics are given in references 7 and 8. The nonlinear six degrees of freedom simulation model is described in reference 9.

The STOLport runway model used in this study is shown in figure 2. The model conforms to the FAA elevated STOLport as documented in reference 6. An elevated STOLport model was used to provide a worst-case test of the proposed vertical guidance procedures.

The MLS simulation is patterned after the prototype MLS system which was installed for flight test evaluations at Crows Landing Navy Auxillary Landing Field, California. This system has a conical elevation beam and a planar azimuth beam. Locations of the antennas relative to the runway are shown in figure 3. The righthand rectangular coordinate system is defined with the origin on the runway opposite the elevation antenna site. The defining equations for the MLS signals as computed in the simulation computer are as follows:

$$\text{DME:} \quad R = ((X-XAZ)^2 + Y^2 + (Z-ZAZ)^2)^{1/2}$$

$$\text{Azimuth:} \quad \psi_M = -\tan^{-1}(Y/(X-XAZ))$$

$$\text{Elevation:} \quad \varepsilon = -\tan^{-1}((Z-ZEL)/(X^2 + (Y-YEL)^2)^{1/2})$$

Where

X, Y, Z = coordinates of airplane

XAZ = X-coordinate of the azimuth antenna and DME, 1363.7m (4474 ft)

ZAZ = Z-coordinate of the azimuth antenna and DME, -1.7m, (-5.5 ft)

YEL = Y-coordinate of the elevation antenna, -73.2 m (-240 ft)

ZEL = Z-coordinate of the elevation antenna, -2.4 m (-7.9 ft)

The simulation program has capabilities for adding biases (randomly selected for each approach) and noise (white or first order correlated noise). Derived signals are transmitted serially to the digital flight control system's computer within its 50 millisecond compute cycle.

The digital flight control system provides various levels of navigation, guidance, control, and pilot interface functions. Reference 5 describes the various system capabilities in detail. The function of interest in this study is the automatic guidance and control during glide slope track and flare to touchdown. The features of the longitudinal axis control law pertinent to this study are briefly described in the next section. A more detailed discussion is given in references 3 and 4, along with a description of the lateral control law.

Longitudinal Axis Control Law

The longitudinal axis control system is shown in figure 4a. Flight path angle is controlled with engine RPM with aid from the faster responding direct lift control (DLC) chokes. Long term airspeed trim is controlled with the elevator with short term control provided by the vectorable nozzles. The throttles, nozzles, and pitch attitude are preset using trim

tables, with deviations from trim corrected by the closed loop control laws. Outputs from the trim tables are constant below 91 meters (300 feet).

During glide slope track, estimates of glide slope deviation and rate are produced by a glide slope complementary filter. Inputs to this filter are raw glide slope deviation derived from elevation and range information and vertical acceleration. The glide slope error is faded out prior to flare. A sink rate estimate used in flare is produced in the sink rate complementary filter. In the flight and simulator evaluation described in reference 4, radar altitude and vertical acceleration were inputs to this sink rate filter. The commanded h/h-dot profile is a straight line from the preflare sink rate to the desired value for touchdown, beginning at altitude of 15.2 meters (50 feet), figure 4b. Flare is initiated at a gear height of 19.8 meters (65 feet) when pitch attitude begins to change from preflare state to the desired touchdown value in a linear manner.

Simulation Conditions

Data for this study were taken with the following conditions:

* -7.5 degree glide slope
* Initialization at X = -4572 m (-15,000 ft), Y = 0, Z = -415m (-1360 ft)
* Avionics system initialized for automatic capture and track of glide slope and automatic flare
* Airspeed of 70 knots
* Approach terminated automatically at touchdown
* No wind or turbulence
* 30 to 35 runs for each MLS error condition

The effects of MLS bias errors were evaluated by conducting three series of about 30 approaches each for the cases (1) no biases introduced, (2) biases introduced on elevation only and (3) biases introduced on DME only. The elevation and DME biases were randomly selected according to the criteria shown in Table I. Larger elevation biases than proposed for operational systems were allowed for the simulator tests to determine the limits of acceptability for the system. For comparison, the biases proposed for operational systems are also shown in Table I. Random noise, (also shown in Table I) was used in all three cases except for some baseline data approaches where no noise or bias were simulated.

The bias error specification which has been proposed for the MLS elevation signal in Table I was obtained from reference 10. In that paper, the bias-type errors are described as Path Following Errors (PFE). A maximum PFE of 0.55 meter (1.8 feet), (2σ) vertical error due to the elevation signal at the 15.2 meter (50 feet) Minimum Guidance Altitude (MGA) was determined. For the CTOL glide slope of 2.7 degrees, the 15.2 meter (50 feet) MGA is about 305 meters (1000 feet) from the elevation antenna. At

that distance the angular PFE is computed to be 0.103 degrees. For the STOL glide slope of 7.5 degrees used in this study, the equivalent 0.55 meter (1.8 feet) maximum vertical error at an altitude of 15.2 meters (50 feet) corresponds to an angular error of 0.27 degrees. According to reference 10, the noise characteristics specification for the elevation signal has not been defined for tightly coupled, precision approaches. Reference 11 proposes that the precision DME system accuracy (with 95-percent probability) be 30.5 meters (100 feet) PFE and 12.2 meters (40 feet) Control Motion Noise (CMN) at the 15.2 meters (50 feet) MGA location. This specification is proposed for both CTOL and STOL systems.

Criteria

The intent of the simulator test program was to examine the control system response and the effects of MLS errors when transitioning from MLS derived altitude to radar altitude during flare. Touchdown rate and location is plotted as a function of both DME and elevation bias errors in order to understand their impact on system performance. The data acquisition was designed to establish trends rather than provide a certification-level evaluation of the control system.

MODIFICATIONS TO LONGITUDINAL CONTROL LAW

Altitude Requirement

A major requirement for successful flare guidance is the accurate measurement of altitude relative to the runway. As discussed earlier, this measurement can most reliably be made using MLS elevation and range signals before reaching the end of the runway surface. Referring to figure 3, for a planar elevation signal the altitude can be computed simply by

$$h = R_{TD} \tan\varepsilon$$

where h = altitude, R_{TD} = range to GPIP, ε = measured elevation angle. Because the elevation antenna installed at Crows Landing and modeled for this study produces a conical beam pattern rather than a planar pattern, this equation would introduce an error in the derived altitude. The conicity error in the derived altitude would be significantly large at altitudes below 30.5 meters (100 feet) in the region where high accuracy is required. The equations necessary to derive the X, Y, Z position of the airplane in the rectangular coordinate system from the conical elevation angle are highly nonlinear and a closed form solution to the equations is very difficult. An approximation method has been developed and tested (ref. 12) which gives an accurate position measurement, minimizing the conicity errors. The method has two steps as follows:

(1) Using the previous Z estimate and the current MLS azimuth and range measurements, compute X and Y.

(2) Then using the filtered X and Y estimates and the current elevation angle measurement, compute the altitude Z.

The coordinate system is shown in figure 3. The equations for the X and Y position determination using this method are:

$$X = XAZ - (R^2 - (ZAZ)^2)^{1/2} \cos \psi$$

$$Y = -(R^2 - (Z - ZAZ)^2)^{1/2} \sin\psi$$

and for altitude from MLS

$$h_{MLS} = - (X^2 + (Y - YEL)^2)^{1/2} \tan\varepsilon + ZEL$$

During glide slope track and flare initiation,

$$Z = -h_{MLS}$$

after transition to radar altimeter,

$$Z = -h_{RA}$$

where h_{RA} is the altitude measured by the radar altimeter.

Transition

Since the latter part of the flare maneuver occurs after the airplane passes out of the approach elevation coverage, a transition to radar altimeter must occur prior to loss of elevation signal. The prototype MLS system at Crows Landing (ref. 1) provides an approach elevation signal that is usable down to about 6 meters (20 feet) above runway level and has usable horizontal coverage of about +65 to +70 degrees from the antenna. Examination of the 7.5 degree elevation glide slope marked on figure 5 shows that the elevation signal should be valid from the end of the runway surface at X = -79.2 meters (-260 feet) to X = -27.4 meters (-90 feet) at 6.1 meters (20 feet) altitude. Thus, the airplane is simultaneously within both MLS elevation signal coverage and over the runway where radar altimeter is usable for about 51.8 meters (170 feet). This condition provides an opportunity for transition from MLS derived altitude to radar altitude.

Examination of the longitudinal control law (figure 4) indicates the requirements for measurement of altitude. During glide slope track, altitude derived from MLS is used to compute the glide slope track error h_{GS} and for initializing the calculation of sink rate using a complementary filter for use during flare (reference 4). The next use of measured altitude is for initiating and controlling the flare maneuver. This is accomplished by use of the numerous gain schedulers which compute commands for sink rate and pitch attitude as functions of altitude. In the original mechanization altitude was provided by the radar altimeter. Flare begins with pitch rotation starting at 19.8 meters (65 feet). Sink rate arrest starts at 15.2 meters (50 feet). Since, as previously mentioned, the airplane on a 7.5 degree glide slope passes over the end of the runway at 12.8 meters (42 feet) altitude and passes out of MLS elevation coverage at about 6.1 meters (20 feet) altitude, transition to a radar altitude reference must occur during the flare maneuver.

Two methods have been identified for transitioning from MLS derived altitude to radar altitude. The simpler method is simply to switch. An alternative is a blending transition. The switch is acceptable as long as a

negligible bias exists between the two altitude measurements. In reality, some bias will normally exist because of errors in the MLS signals and in the radar altimeter. If a switch were to occur at the landing threshold (at X = -48.8 meters (-160 feet)) and an elevation error of 0.05 degree and DME error of 12.2 meters (40 feet) were present, the derived altitude would be in error by about 1.7 meters (5.5 feet). The control law is sensitive to instantaneous altitude measurement changes which tend to produce undesirable, rapid control response.

The more preferable solution, therefore, appears to be a slower, blending transition. The criteria for controlling this blending can be either altitude or distance along the runway. The use of altitude has the disadvantage of having the location along the runway shift as different glide slopes are selected, possibly moving the transition to a location where one or the other signal is lost for part of the blend. Since limiting the transition zone to a specific section of the runway is important, the test for switching from MLS altitude to radar altitude is best based on either raw DME or computed distance along the runway, which in turn strongly depends on DME. Distance along the runway (X coordinate, figure 3) is available from the navigation subsystem of the digital flight control system being used, so it was used as the control parameter for this study.

Since the MLS elevation signal will be available over the runway from X = -79.2 meters (-90 feet), the blending transition can be done over this distance. If the determination of X is in error, however, part of the transition would move into a region where either the radar altimeter may have large errors or the elevation signal is lost. Either situation could put large errors into the altitude calculation and, therefore, transients into the control system. Near touchdown, the X-position is primarily dependent on the DME. Since bias error in the DME is expected to be at least 15.2 meters (50 feet) on a 2-sigma basis, a transition zone of 15.2 to 18.2 meters (50 to 60 feet) appears to be the maximum distance available. For the simulator tests, the transition zone was between X = -64.0 m (-210 feet) and X = -45.7 m (-150 feet). To provide a gradual shift from MLS to radar altitude, the following blending equations were used for altitude,

$$h_{BL} = (h_{RA}) - \left[\frac{X - (-46)}{-64 - (-46)}\right](h_{RA} - h_{MLS})$$

and $$Z = -h_{BL}$$

An example of this blending transition is shown in figure 6.

Sink Rate Requirement

Flare monitoring systems and control laws for flare guidance typically require an accurate determination of vertical velocity, or sink rate. The flare guidance system used in this study uses the derived sink rate to produce an error signal from a commanded sink rate profile, figure 4b. The commanded sink rate decreases linearly with altitude from the existing preflare sink rate at 15.2 meters (50 feet) to the desired touchdown value. The result is an exponential flare. Prior to flare, the glide slope track control law uses a vertical rate error relative to the glide slope. Gain schedulers transition the derived sink rate linearly from glide slope to altitude based information throughout the flare. This tends to minimize the

impact of small terrain irregularities. A more complete description of this flare law implementation is given in reference 4.

Sink rate was originally determined in this system by blending the radar altitude with vertical acceleration in a complementary filter, figure 7, starting at 152 meters (500 feet) above ground level when the precision radar altitude signal became valid. This procedure was successful because (a) 1372 meters (4500 feet) of runway was available short of the STOLport markings and (b) the sink rate filter was converged long before the estimate was needed to begin the flare. The filter was initialized at glide slope capture and computed the vertical rate until touchdown. For this study, the use of MLS derived altitude was the input to the filter until the airplane was over the STOLport runway where the radar altitude could provide a valid reference. Use of the altitude reference with blending transition from MLS to radar altimeter, described previously, was investigated. During the blending an erroneous sink rate is detected if a bias exists between the MLS and radar altitudes. The effect on the complementary filter is to produce a large transient in the output which takes several seconds to decay. For a bias of about 1.5 meters (5 feet) (figure 8a), the response is as shown in figure 8b. To prevent the transient, a procedure was developed to compute the bias between the MLS and radar altitudes after the airplane is over the runway while MLS-derived altitude is used as input to the filter. Then, as shown in figure 7, the filter input h_{SR}, was switched to radar altitude plus the computed bias. This procedure removes the erroneous rates from the filter input and produces the response shown in figure 8c. For programming convenience, the bias was computed during the altitude blending interval with the altitude input to the filter being switched at the end of the blending interval. Note that the biased altitude described here is used only for computation of an accurate, transient-free sink rate during flare, not as the altitude measurement.

RESULTS AND DISCUSSION

An evaluation of the proposed implementation was conducted in the fixed-base STOL simulator described previously. The effect on the control system of the transition from MLS-derived altitude to radar altitude was determined by changes in the touchdown sink rate and touchdown distance along the runway. Since the primary disturbance to the system during the transition comes from biases in the MLS elevation and DME signals, the system performance was tested with a variety of biases. The control system produced the statistical results shown in Table II. Graphical presentations of these data are shown in figures 9 and 10, where the cumulative percent of occurrences are plotted for each bias condition. The straight lines are drawn through the mean and $\pm$ 1-sigma values and the individual touchdown data are marked.

Because of the fundamental control system requirement to provide a tightly controlled sink rate, the sink rate at touchdown is not affected significantly by biases, figure 9. Therefore, the mean sink rate at touchdown was essentially identical for all three test conditions. The standard deviation is somewhat higher for the elevation biases. There is more variation in touchdown distance between the bias conditions. The touchdown distances for the elevation biases were similar to the no-bias

flights. However, the DME bias conditions encountered produced a wider variation in touchdown distance, figure 10. The longer mean touchdown distance may be caused at least partially by the DME biases between +15.2 meters (+50 feet) and +25.9 meters (+85 feet), which were used to test their effect on the control system. Biases longer than -15.2 meters (-50 feet) were eliminated because they caused initiation of the MLS to radar transition before the end of the runway and thus the large radar altimeter error introduced large transients into the control system.

Correlation between the MLS biases and the touchdown states are more easily seen in Figures 11 and 12. The least squares straight line fit to the data points are shown as a solid line in the plots. There is some correlation of sink rate and touchdown distance with the elevation bias, Figure 11. However, the limits of the elevation biases used in the tests were much larger than expected in operational systems. At small elevation biases, no significant correlation appears to exist between either sink rate or touchdown distance and biases in the elevation signal. This result was expected, since, for small biases, the vertical error is very small at the short distances involved during the flare maneuver and the high bandwidth sink rate control system was able to eliminate the error before touchdown.

Figure 12 shows that there is no correlation between sink rate and DME bias. However, touchdown dispersions do correlate with DME bias errors. Positive biases cause the derived distance along the runway to be further out than the actual distance. Likewise, the derived altitude is higher than the actual altitude before the transition to radar altitude is made. These errors cause the flare maneuvers to be started lower and further along the runway than normal. The control system used in the test had the bandwidth necessary to arrest the sink rate to the value commanded for touchdown. Starting the flare late along the runway merely caused the touchdown to be further down the runway. Negative biases produce correspondingly shorter touchdowns. For maximum DME biases of $\pm$ 15.2 meters (+ 50 feet) or less, the touchdown dispersion is not excessive. The data recorded where DME biases were between +15.2 meters (50 feet) and 25.9 meters (85 feet) generally follow the trends set where the biases were in the +15.2 meters (+ 50 feet) range. At the longer positive biases, the transition zone is moved toward the GPIP and into a region where the elevation signal may be lost. In the simulator, the signal was assumed to be valid; and, since the radar altimeter was valid, no transients were introduced into the system. As noted previously, negative DME biases longer than 15.2 meters (50 feet) produced unsatisfactory results and so are not plotted in figure 12.

From the data presented, small MLS elevation and DME biases and noise do not appear to present any significant problems for the proposed procedures of transitioning from MLS derived altitude to radar altimeter during the flare maneuver. The autoland system used in the evaluation had enough bandwidth to hold the sink rate at touchdown within close limits. Touchdown distance was not a feedback parameter in the control system and thus tended to be more variable than sink rate. Other system designs may differ in their response to the altitude reference errors which can occur during the flare maneuver. However, the altitude and longitudinal distance estimate errors will be small, particularly at the two-sigma level of

elevation and DME biases recommended for operational MLS systems at STOLports.

The MLS specifications which have been proposed for CTOL runways appear to be adequate for STOLports with one or two exceptions. While the proposed approach elevation accuracy specifications appear satisfactory, coverage of the signal over the runway in the flare zone limits the distance available for the altitude reference transition. The coverage assumed for the simulator tests appears to be adequate. Care should be taken in the development of operational systems to provide at least a similar coverage. A more critical specification is the DME Path Following Error (bias). The 30.5 meters (100 feet) (2 σ) proposed PFE does not allow sufficient distance to transition from MLS derived altitude to a radar altitude. For the STOLport geometry proposed by the FAA and used in this study, a maximum PFE (improbable event level) of $\pm$ 15.2 meters (+ 50 feet) is required. This interpolates to about 6.1 meters (20 feet) at 95% probability level. Some relaxation of this tight specification could be made by moving the approach elevation antenna further down the runway at the expense of reducing the available stopping distance. A second alternative is lengthening the underrun, now set at 30.5 meters (100 feet). Extending the underrun to at least 80 meters (260 feet) would be required to safely accommodate a PFE of 30.5 meters (100 feet).

Although no pilot evaluation of the modified system was made, the landing performance data compared favorably with that obtained during flight testing of the unmodified system over an extended runway surface. Those flight tests indicated that the repeatability consistency of performance obtained is acceptable to pilots for normal aircraft operation.

CONCLUSIONS

A modification to a conventional autoland system has been developed which allows the use of MLS for initiation of an automatic flare maneuver by a STOL airplane. After initiation of the flare using MLS and after crossing the threshold, a transition can be made to radar altimeter with a minimum effect on the control system response. A blending transition from MLS to radar altimeter is quite adequate for the altitude reference. The procedure of switching from MLS derived altitude to a biased radar altitude as input to the sink rate filter has been shown to provide an accurate, transient-free vertical velocity for use in the flare control algorithm.

The MLS specifications proposed for CTOL operations proved to be acceptable for STOLport operations with the exception of the DME Path Following Error (bias) specification. The 30.5 meters (2 σ) proposed PFE for CTOL systems should be reduced to about 6 meters for satisfactory automatic landings, particularly on an elevated STOLport runway.

Based on these simulation results, the autoland procedure developed in this study is capable of producing repeatable, consistent performance which should be accepable for normal operation.

References

1. Hodgkins, P.D.; and Cafarelli, N.J.: Design Considerations for a Flare Guidance System. NAVIGATION: Journal of the Institute of Navigation, vol. 23, no. 3, Fall 1976.

2. Lambregts, A.A.; and Creedon, J.F.: Development and Flight Evaluations of Automatic Flare Laws with Improved Touchdown Dispersion. AIAA Guidance and Control Conference, Paper No. 80-1757, Danvers, Mass., August 11-13, 1980.

3. Feinreich, B.; Gevaert, G.; Hardy, G.H.; and Watson, D.M.: Development of Automatic Landing Control Laws for Powered Lift Short Haul Aircraft. AIAA Paper No. 80-1759, August 1980.

4. Feinreich, B.; and Gevaret, G.: Development and Evaluation of Automatic Landing Control Laws for Powered Lift STOL Aircraft. NASA CR 152399, Jan. 1981.

5. Neuman, F.; Watson, D.M.; Bradbury, P.: Operational Description of an Experimental Digital Avionics System for STOL Airplanes. NASA-TMX-62,448, 1975.

6. Anon.: Planning and Design Criteria for Metropolitan STOL Ports. FAA Advisory Circular 150/5300-8, Nov. 1970.

7. Quigley, H.C.; Innis, R.C.; and Grossmith, S.: A Flight Investigation of the STOL Characteristics of an Augmented Jet Flap STOL Research Aircraft. NASA TMX-62,334, May 1974.

8. Hindson, W.S.; Hardy, G.H.; and Innis, R.C.: Evaluation of Several STOL Control and Flight Director Concepts from Flight Tests of a Powered-Lift Aircraft Flying Steep, Curved Approaches. NASA TP 1641, March 1981.

9. Cleveland, W.B.; Vomaske, R.F.; and Sinclair, S.R.M.: Augmentor Wing Jet STOL Research Aircraft Simulation Model. NASA TMX-62,149, April 1972.

10. Kelly, R.J.: Guidance Accuracy Considerations for the Microwave Landing System. NAVIGATION: Journal of the Institute of Navigation, Vol. 24, No. 3, Fall 1977.

11. Kelly, R.J.; and LeBerge, E.F.C.: Guidance Accuracy Considerations for the Microwave Landing System Precision DME. NAVIGATION: Journal of the Institute of Navigation, vol. 27, no. 1, Spring 1980.

12. Neuman, R.; and Warner, D.N. Jr.: A STOL Terminal Area Navigation System. NASA TMX-62,348, May 1974.

TABLE I: MLS ERROR COMBINATIONS

Error Combination	Function	Units	Bias (2σ)	Noise (2σ)
Test	EL	deg	0.5	.03
Conditions	DME	m	30.5	12.2
B				
Proposed	EL	deg	0.27	0.05
Specs	DME	m	30.5	12.2

TABLE II: TOUCHDOWN STATISTICS

		h_{TD} (m/sec)		x_{TD} (m)	
Condition	No. of Approaches	Mean	Sigma	Mean	Sigma
No biases	32	1.1	0.04	99.7	4.6
Elevation biases	34	1.1	0.06	99.4	5.8
DME biases ($\pm$50.2m)	24	1.1	0.04	101.2	7.3
DME biases (-15.2m) (+30.5m)	30	1.1	0.04	103.9	9.1

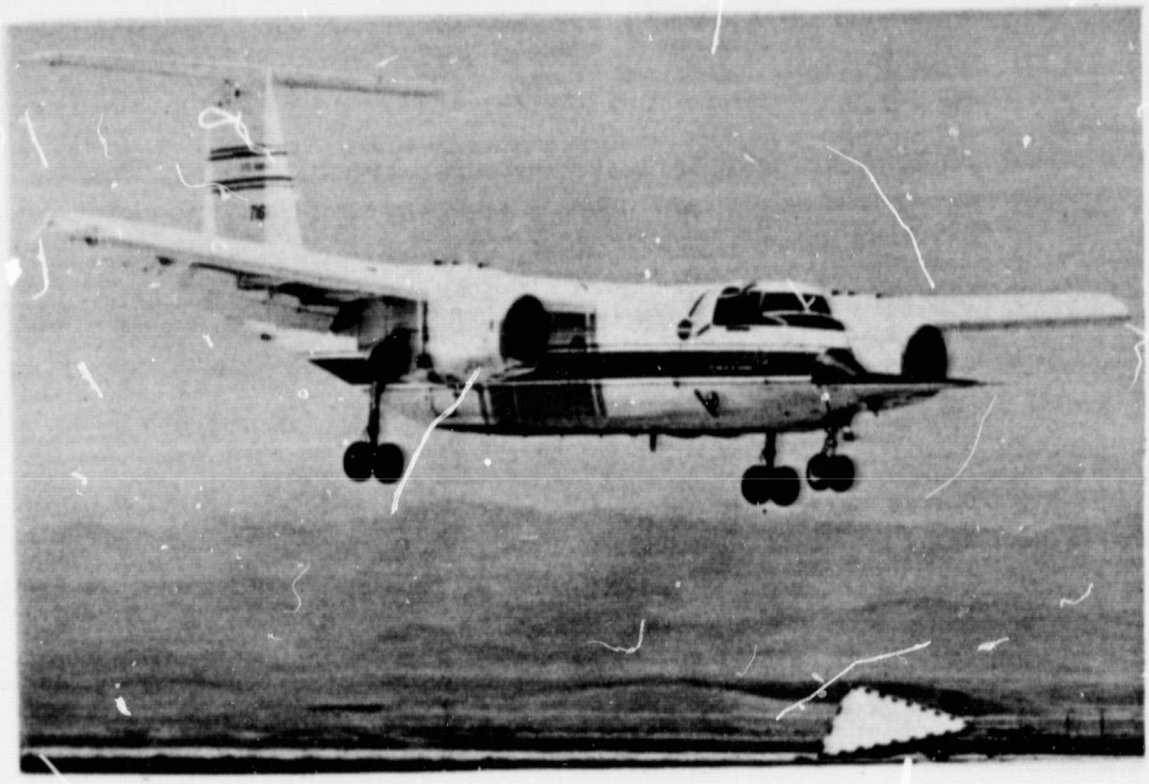

Figure 1.- Augmentor wing jet STOL research aircraft.

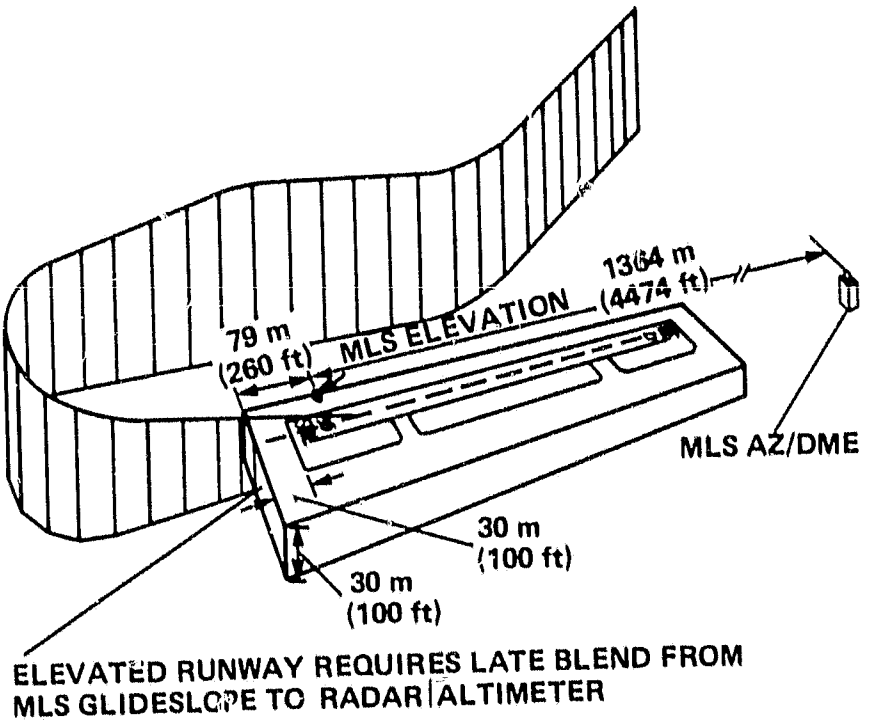

Figure 2.- Elevated STOLport runway.

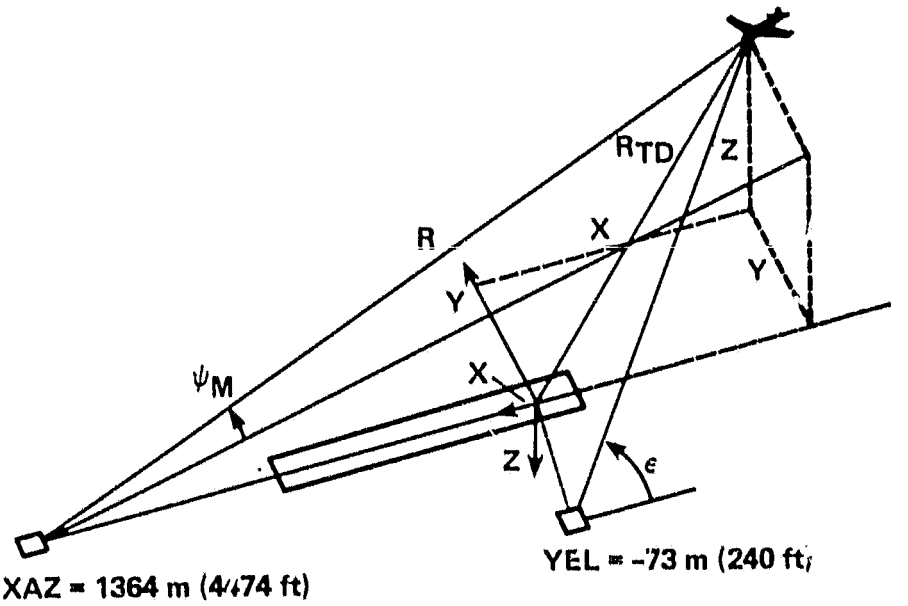

Figure 3.- Geometry of MLS antennas using a runway-oriented system.

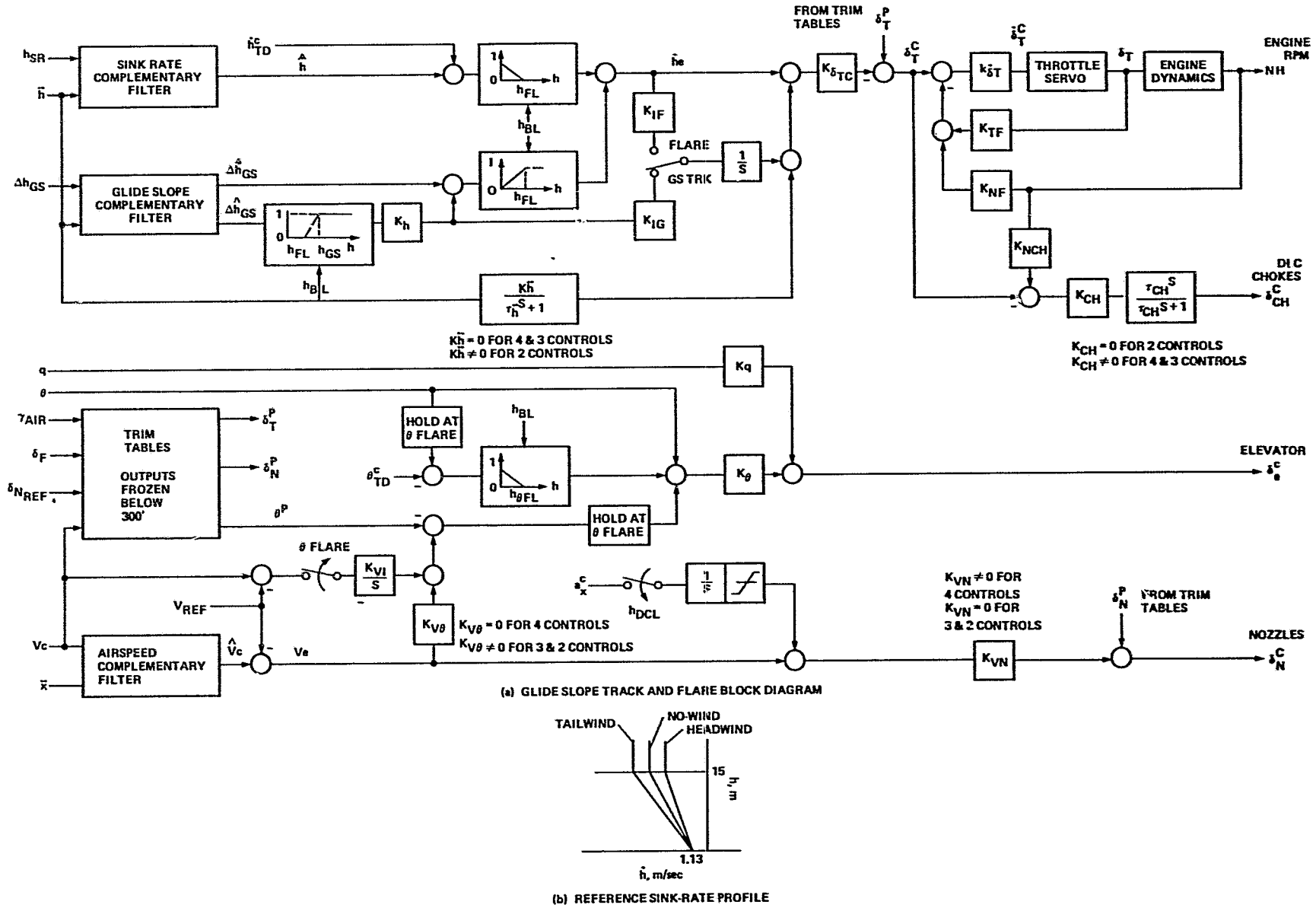

Figure 4.- (a) Glide slope track and flare block diagram. (b) Reference sink-rate profile.

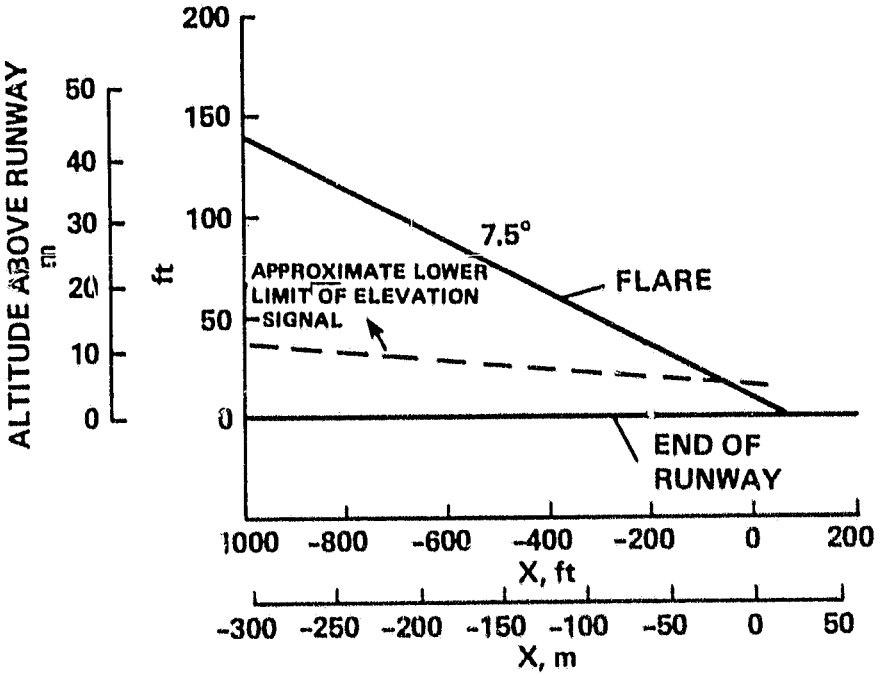

Figure 5.- MLS elevation signal coverage.

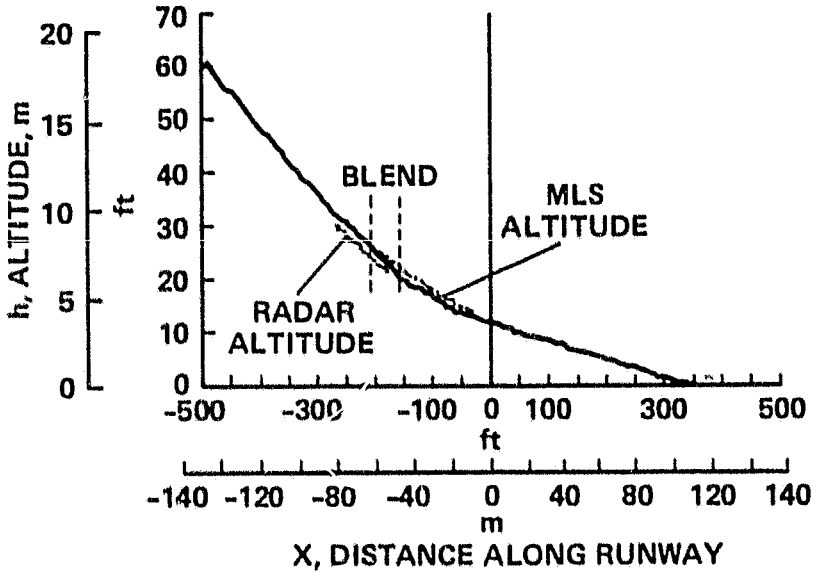

Figure 6.- Blending transition from MLS to radio altitude (20 ft DME bias).

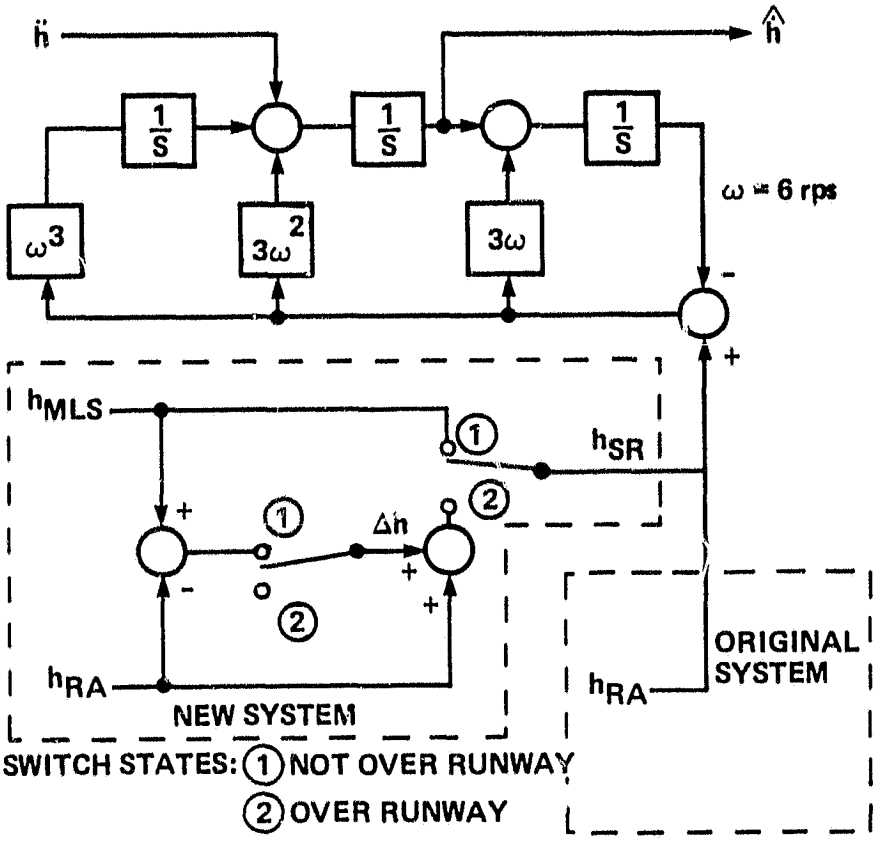

Figure 7.- Sink rate complementary filter.

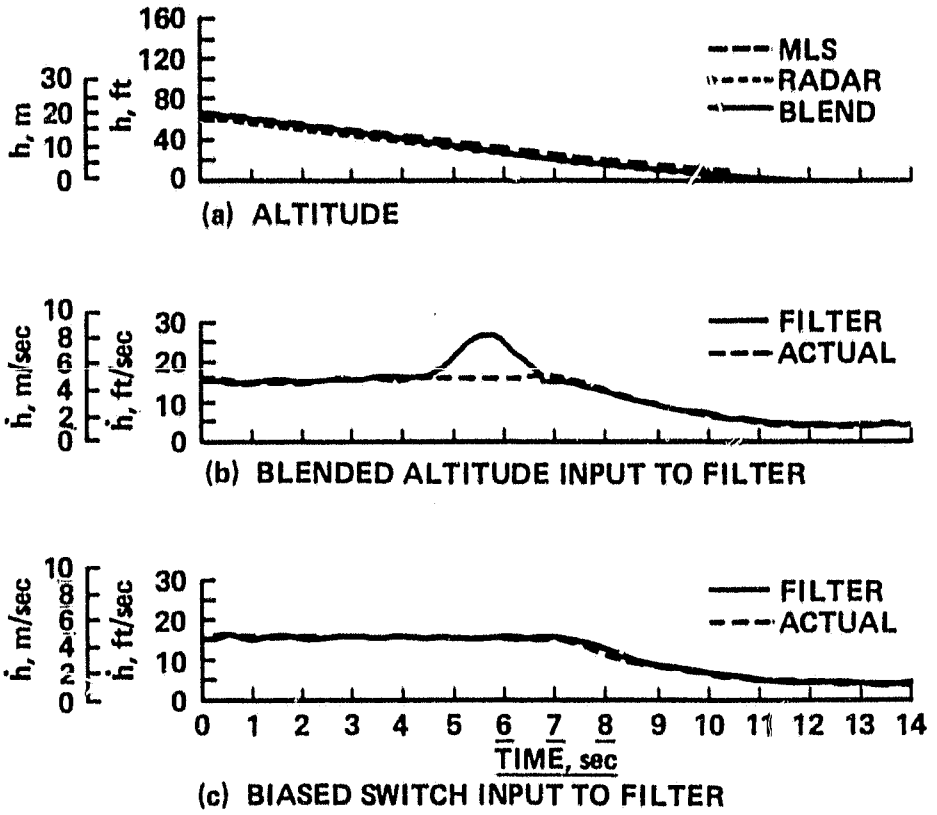

Figure 8.- Sink rate filter response.

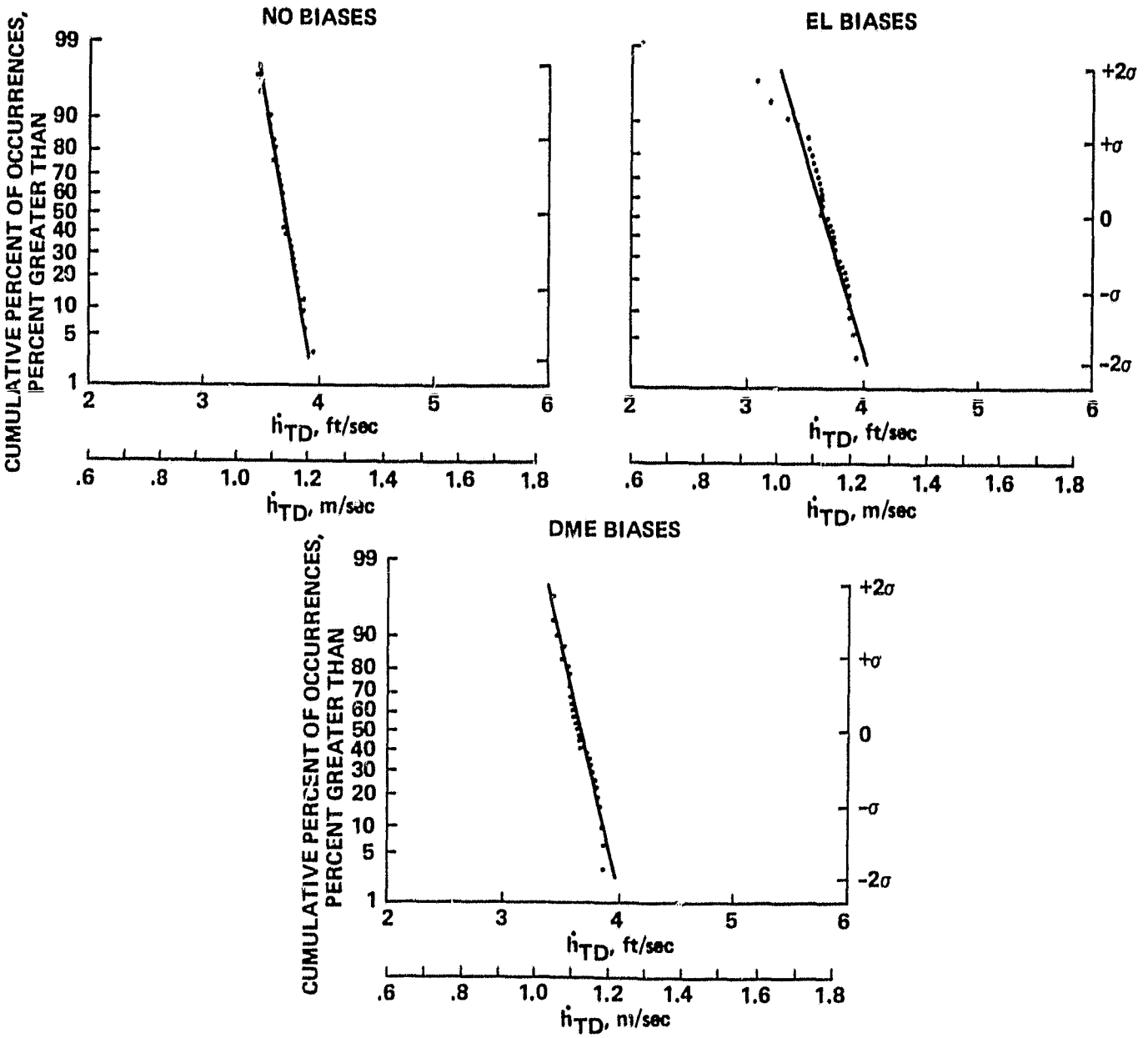

Figure 9.- Sink rate at touchdown.

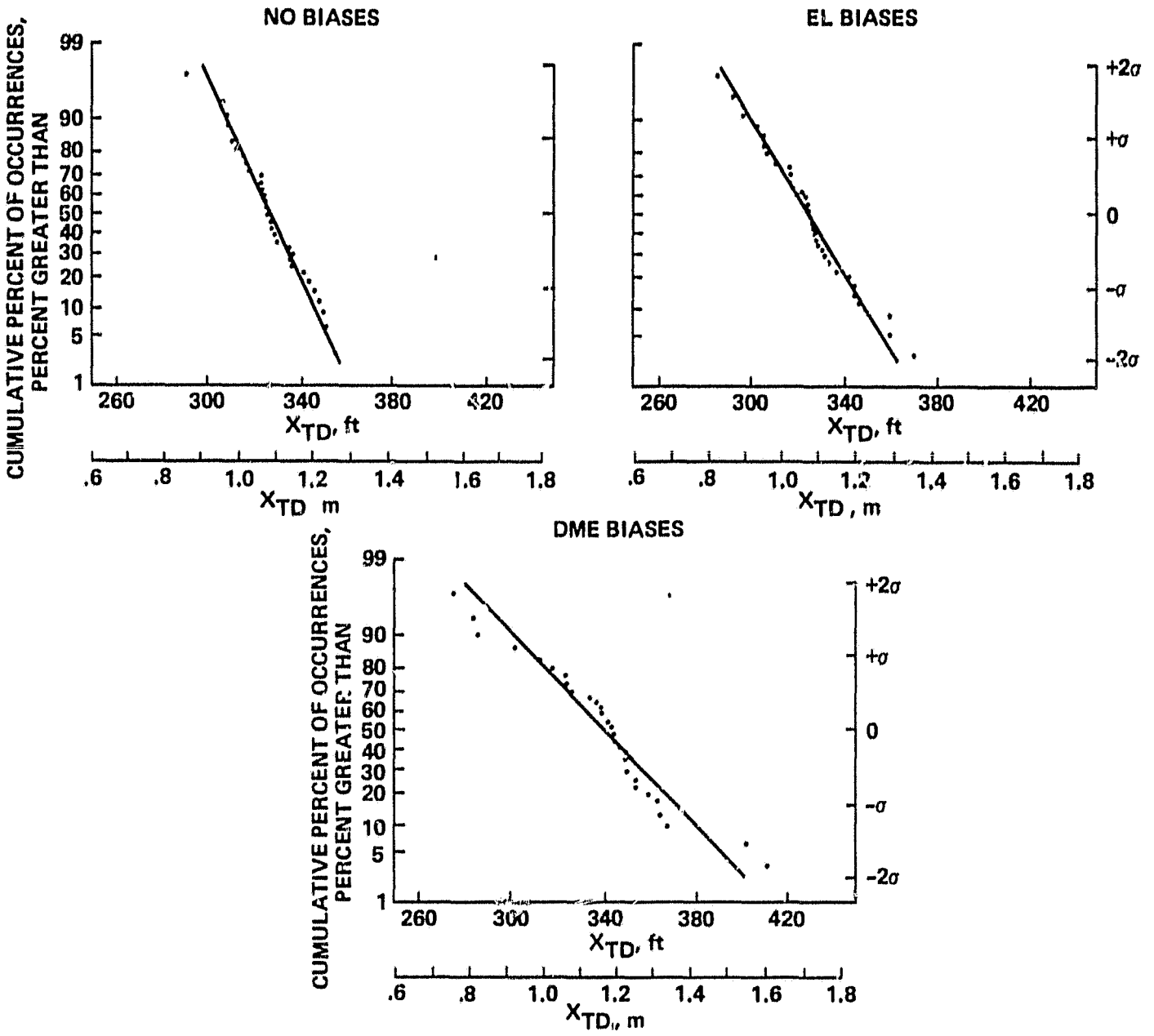

Figure 10.- Distance along runway at touchdown.

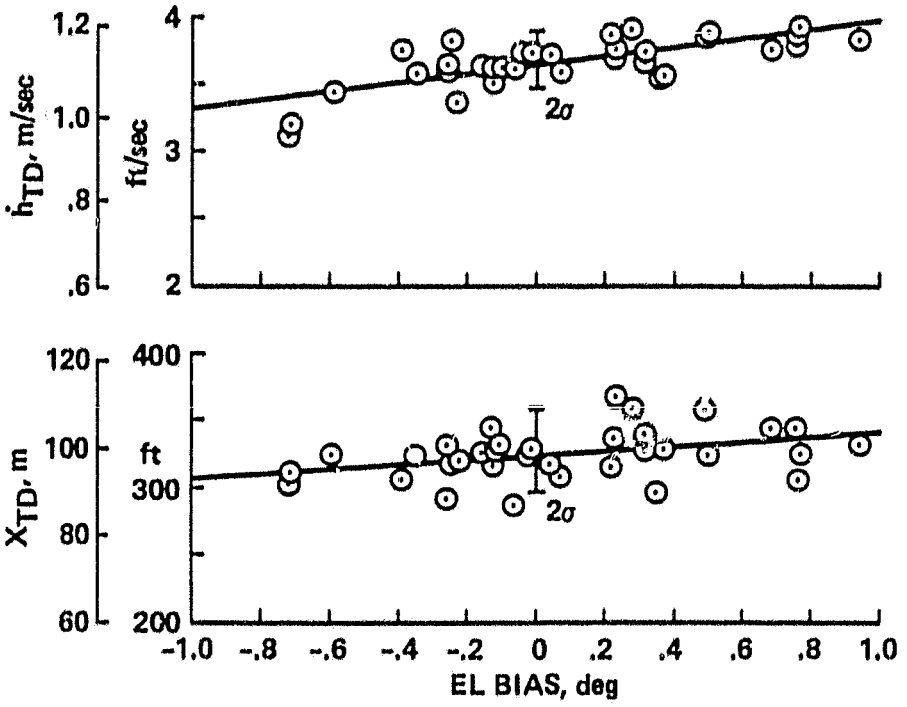

Figure 11.- Elevation biases.

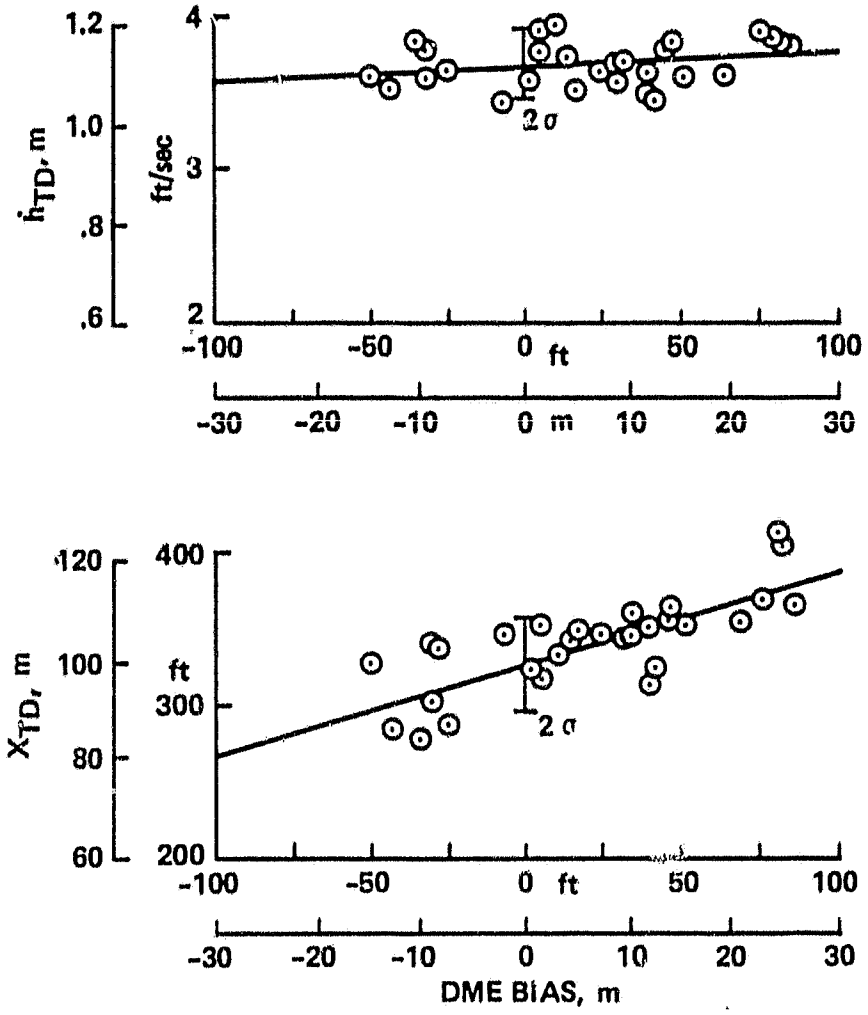

Figure 12. DME biases.